Atomic and Electronic Structure of Solids

Efthimios Kaxiras

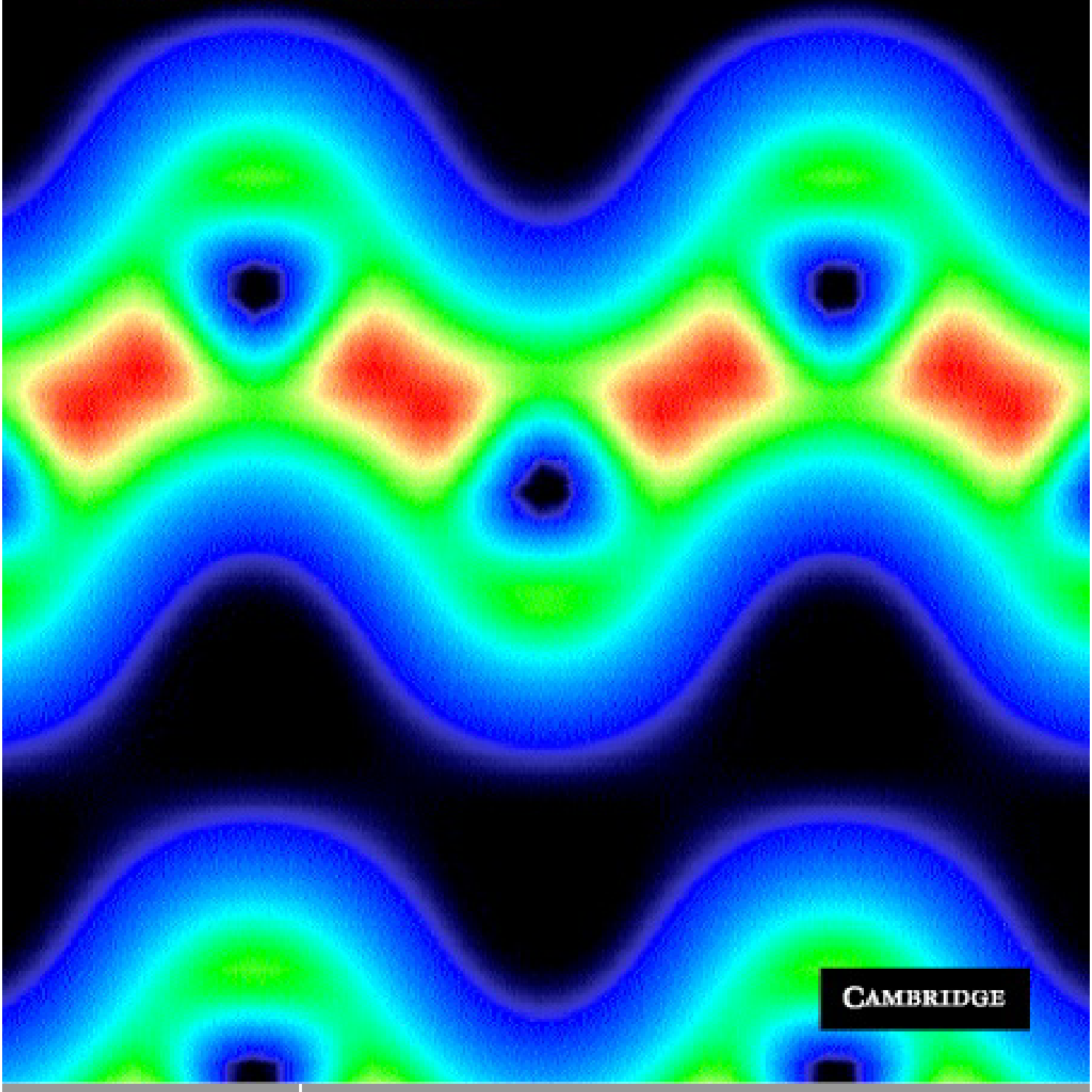

CAMBRIDGE

CAMBRIDGE

more information - www.cambridge.org/9780521810104

4

Band structure of crystals

In the previous two chapters we examined in detail the effects of crystal periodicity and crystal symmetry on the eigenvalues and wavefunctions of the single-particle equations. The models we used to illustrate these effects were artificial free-electron models, where the only effect of the presence of the lattice is to impose the symmetry restrictions on the eigenvalues and eigenfunctions. We also saw how a weak periodic potential can split the degeneracies of certain eigenvalues at the Bragg planes (the BZ edges). In realistic situations the potential is certainly not zero, as in the free-electron model, nor is it necessarily weak. Our task here is to develop methods for determining the solutions to the single-particle equations for realistic systems. We will do this by discussing first the so called tight-binding approximation, which takes us in the most natural way from electronic states that are characteristic of atoms (atomic orbitals) to states that correspond to crystalline solids. We will then discuss briefly more general methods for obtaining the band structure of solids, whose application typically involves a large computational effort. Finally, we will conclude the chapter by discussing the electronic structure of several representative crystals, as obtained by elaborate computational methods; we will also attempt to interpret these results in the context of the tight-binding approximation.

4.1 The tight-binding approximation

The simplest method for calculating band structures, both conceptually and computationally, is the so called Tight-Binding Approximation (TBA), also referred to as Linear Combination of Atomic Orbitals (LCAO). The latter term is actually used in a wider sense, as we will explain below. The basic assumption in the TBA is that we can use orbitals that are very similar to atomic states (i.e. wavefunctions tightly bound to the atoms, hence the term "tight-binding") as a basis for expanding the crystal wavefunctions. We will deal with the general theory of the TBA first, and then we will illustrate how it is applied through a couple of examples.

Suppose then that we start with a set of atomic wavefunctions

$$\phi_l(\mathbf{r} - \mathbf{t}_i) \tag{4.1}$$

where $\mathbf{t}_i$ is the position of atom with label i in the PUC, and $\phi_l(\mathbf{r})$ is one of the atomic states associated with this atom. The index l can take the usual values for an atom, that is, the angular momentum character $s, p, d, \ldots$. The state $\phi_l(\mathbf{r} - \mathbf{t}_i)$ is centered at the position of the atom with index i. It is assumed that we need as many orbitals as the number of valence states in the atom (this is referred to as the "minimal basis").

Our first task is to construct states which can be used as the basis for expansion of the crystal wavefunctions. These states must obey Bloch's theorem, and we call them $\chi_{\mathbf{k}li}(\mathbf{r})$:

$$\chi_{\mathbf{k}li}(\mathbf{r}) = \frac{1}{\sqrt{N}} \sum_{\mathbf{R}'} \mathrm{e}^{\mathrm{i}\mathbf{k}\cdot\mathbf{R}'} \phi_l(\mathbf{r} - \mathbf{t}_i - \mathbf{R}') \tag{4.2}$$

with the summation running over all the N unit cells in the crystal (the vectors $\mathbf{R}'$), for a given pair of indices i (used to denote the position $\mathbf{t}_i$ of the atom in the PUC) and l (used for the type of orbital). We first verify that these states have Bloch character:

$$\begin{aligned}
\chi_{\mathbf{k}li}(\mathbf{r} + \mathbf{R}) &= \frac{1}{\sqrt{N}} \sum_{\mathbf{R}'} \mathrm{e}^{\mathrm{i}\mathbf{k}\cdot(\mathbf{R}'-\mathbf{R})} \mathrm{e}^{\mathrm{i}\mathbf{k}\cdot\mathbf{R}} \phi_l((\mathbf{r} + \mathbf{R}) - \mathbf{t}_i - \mathbf{R}') \\
&= \mathrm{e}^{\mathrm{i}\mathbf{k}\cdot\mathbf{R}} \frac{1}{\sqrt{N}} \sum_{\mathbf{R}'} \mathrm{e}^{\mathrm{i}\mathbf{k}\cdot(\mathbf{R}'-\mathbf{R})} \phi_l(\mathbf{r} - \mathbf{t}_i - (\mathbf{R}' - \mathbf{R})) \\
&= \mathrm{e}^{\mathrm{i}\mathbf{k}\cdot\mathbf{R}} \frac{1}{\sqrt{N}} \sum_{\mathbf{R}''} \mathrm{e}^{\mathrm{i}\mathbf{k}\cdot\mathbf{R}''} \phi_l(\mathbf{r} - \mathbf{t}_i - \mathbf{R}'') = \mathrm{e}^{\mathrm{i}\mathbf{k}\cdot\mathbf{R}} \chi_{\mathbf{k}li}(\mathbf{r})
\end{aligned} \tag{4.3}$$

that is, Bloch's theorem is satisfied for our choice of $\chi_{\mathbf{k}li}(\mathbf{r})$, with the obvious definition $\mathbf{R}'' = \mathbf{R}' - \mathbf{R}$, which is another lattice vector. Now we can expand the crystal single-particle eigenstates in this basis:

$$\psi^{(n)}_{\mathbf{k}}(\mathbf{r}) = \sum_{l,i} c^{(n)}_{\mathbf{k}li} \chi_{\mathbf{k}li}(\mathbf{r}) \tag{4.4}$$

and all that remains to do is determine the coefficients $c^{(n)}_{\mathbf{k}li}$, assuming that the $\psi^{(n)}_{\mathbf{k}}(\mathbf{r})$ are solutions to the appropriate single-particle equation:

$$\mathcal{H}^{sp}\psi^{(n)}_{\mathbf{k}}(\mathbf{r}) = \epsilon_{\mathbf{k}}\psi^{(n)}_{\mathbf{k}}(\mathbf{r}) \Rightarrow \sum_{l,i} \Big[\langle \chi_{\mathbf{k}mj} | \mathcal{H}^{sp} | \chi_{\mathbf{k}li} \rangle - \epsilon^{(n)}_{\mathbf{k}} \langle \chi_{\mathbf{k}mj} | \chi_{\mathbf{k}li} \rangle \Big] c^{(n)}_{\mathbf{k}li} = 0 \tag{4.5}$$

In the above equation we only need to consider matrix elements of states with the same $\mathbf{k}$ index, because

$$\left\langle \psi_{\mathbf{k}}^{(n)} \middle| \psi_{\mathbf{k}'}^{(n')} \right\rangle \sim \delta(\mathbf{k} - \mathbf{k}') \tag{4.6}$$

where we are restricting the values of $\mathbf{k}$, $\mathbf{k}'$ to the IBZ. In Eq. (4.5) we have a secular equation of size equal to the total number of atomic orbitals in the PUC: the sum is over the number of different types of atoms and the number of orbitals associated with each type of atom. This is exactly the number of solutions (bands) that we can expect at each $\mathbf{k}$-point. In order to solve this linear system we need to be able to evaluate the following integrals:

$$\begin{aligned}
\langle \chi_{\mathbf{k}mj} | \chi_{\mathbf{k}li} \rangle &= \frac{1}{N} \sum_{\mathbf{R}',\mathbf{R}''} \mathrm{e}^{\mathrm{i}\mathbf{k}\cdot(\mathbf{R}'-\mathbf{R}'')} \langle \phi_m(\mathbf{r} - \mathbf{t}_j - \mathbf{R}'') | \phi_l(\mathbf{r} - \mathbf{t}_i - \mathbf{R}') \rangle \\
&= \frac{1}{N} \sum_{\mathbf{R},\mathbf{R}'} \mathrm{e}^{\mathrm{i}\mathbf{k}\cdot\mathbf{R}} \langle \phi_m(\mathbf{r} - \mathbf{t}_j) | \phi_l(\mathbf{r} - \mathbf{t}_i - \mathbf{R}) \rangle \\
&= \sum_{\mathbf{R}} \mathrm{e}^{\mathrm{i}\mathbf{k}\cdot\mathbf{R}} \langle \phi_m(\mathbf{r} - \mathbf{t}_j) | \phi_l(\mathbf{r} - \mathbf{t}_i - \mathbf{R}) \rangle
\end{aligned} \tag{4.7}$$

where we have used the obvious definition $\mathbf{R} = \mathbf{R}' - \mathbf{R}''$, and we have eliminated one of the sums over the lattice vectors with the factor $1/N$, since in the last line of Eq. (4.7) there is no explicit dependence on $\mathbf{R}'$. We call the brackets in the last expression the "overlap matrix elements" between atomic states. In a similar fashion we obtain:

$$\langle \chi_{\mathbf{k}mj} | \mathcal{H}^{sp} | \chi_{\mathbf{k}li} \rangle = \sum_{\mathbf{R}} \mathrm{e}^{\mathrm{i}\mathbf{k}\cdot\mathbf{R}} \langle \phi_m(\mathbf{r} - \mathbf{t}_j) | \mathcal{H}^{sp} | \phi_l(\mathbf{r} - \mathbf{t}_i - \mathbf{R}) \rangle \tag{4.8}$$

and we call the brackets on the right-hand side of Eq. (4.8) the "hamiltonian matrix elements" between atomic states.

At this point we introduce an important approximation: in the spirit of the TBA, we take the overlap matrix elements in Eq. (4.7) to be non-zero only for the same orbitals on the same atom, i.e. only for $m = l$, $j = i$, $\mathbf{R} = 0$, which is expressed by the relation

$$\langle \phi_m(\mathbf{r} - \mathbf{t}_j) | \phi_l(\mathbf{r} - \mathbf{t}_i - \mathbf{R}) \rangle = \delta_{lm} \delta_{ij} \delta(\mathbf{R}) \tag{4.9}$$

This is referred to as an "orthogonal basis", since any overlap between different orbitals on the same atom or orbitals on different atoms is taken to be zero.[1]

[1] If the overlap between the $\phi_m(\mathbf{r})$ orbitals was strictly zero, there would be no interactions between nearest neighbors; this is only a convenient approximation.

Table 4.1. *Equations that define the TBA model.*

The first three equations are general, based on the atomic orbitals $\phi_l(\mathbf{r}-\mathbf{t}_i-\mathbf{R})$ of type l centered at an atom situated at the position $\mathbf{t}_i$ of the unit cell with lattice vector $\mathbf{R}$. The last three correspond to an orthogonal basis of orbitals and nearest neighbor interactions only, which define the on-site and hopping matrix elements of the hamiltonian.

$\chi_{\mathbf{k}li}(\mathbf{r}) = \frac{1}{\sqrt{N}}\sum_{\mathbf{R}} e^{i\mathbf{k}\cdot\mathbf{R}}\phi_l(\mathbf{r}-\mathbf{t}_i-\mathbf{R})$	Bloch basis
$\psi^{(n)}_{\mathbf{k}}(\mathbf{r}) = \sum_{l,i} c^{(n)}_{\mathbf{k}li}\chi_{\mathbf{k}li}(\mathbf{r})$	crystal states
$\sum_{l,i}\left[\langle\chi_{\mathbf{k}mj}\|\mathcal{H}^{sp}\|\chi_{\mathbf{k}li}\rangle - \epsilon^{(n)}_{\mathbf{k}}\langle\chi_{\mathbf{k}mj}\|\chi_{\mathbf{k}li}\rangle\right]c^{(n)}_{\mathbf{k}li} = 0$	secular equation
$\langle\phi_m(\mathbf{r}-\mathbf{t}_j)\|\phi_l(\mathbf{r}-\mathbf{t}_i-\mathbf{R})\rangle = \delta_{lm}\delta_{ij}\delta(\mathbf{R})$	orthogonal orbitals
$\langle\phi_m(\mathbf{r}-\mathbf{t}_j)\|\mathcal{H}^{sp}\|\phi_l(\mathbf{r}-\mathbf{t}_i-\mathbf{R})\rangle = \delta_{lm}\delta_{ij}\delta(\mathbf{R})\epsilon_l$	on-site elements
$\langle\phi_m(\mathbf{r}-\mathbf{t}_j)\|\mathcal{H}^{sp}\|\phi_l(\mathbf{r}-\mathbf{t}_i-\mathbf{R})\rangle = \delta((\mathbf{t}_j-\mathbf{t}_i-\mathbf{R})-\mathbf{d}_{nn})V_{lm,ij}$	hopping elements

Similarly, we will take the hamiltonian matrix elements in Eq. (4.8) to be non-zero only if the orbitals are on the same atom, i.e. for $j=i$, $\mathbf{R}=0$, which are referred to as the "on-site energies":

$$\langle\phi_m(\mathbf{r}-\mathbf{t}_j)|\mathcal{H}^{sp}|\phi_l(\mathbf{r}-\mathbf{t}_i-\mathbf{R})\rangle = \delta_{lm}\delta_{ij}\delta(\mathbf{R})\epsilon_l \tag{4.10}$$

or, if the orbitals are on different atoms but situated at nearest neighbor sites, denoted in general as $\mathbf{d}_{nn}$:

$$\langle\phi_m(\mathbf{r}-\mathbf{t}_j)|\mathcal{H}^{sp}|\phi_l(\mathbf{r}-\mathbf{t}_i-\mathbf{R})\rangle = \delta((\mathbf{t}_j-\mathbf{t}_i-\mathbf{R})-\mathbf{d}_{nn})V_{lm,ij} \tag{4.11}$$

The $V_{lm,ij}$ are also referred to as "hopping" matrix elements. When the nearest neighbors are in the same unit cell, $\mathbf{R}$ can be zero; when they are across unit cells $\mathbf{R}$ can be one of the primitive lattice vectors. The equations that define the TBA model, with the approximation of an orthogonal basis and nearest neighbor interactions only, are summarized in Table 4.1. Even with this drastic approximation, we still need to calculate the values of the matrix elements that we have kept. The parametrization of the hamiltonian matrix in an effort to produce a method with quantitative capabilities has a long history, starting with the work of Harrison [37] (see the Further reading section), and continues to be an active area of research. In principle, these matrix elements can be calculated using one of the single-particle hamiltonians we have discussed in chapter 2 (this approach is being actively pursued as a means of performing fast and reliable electronic structure calculations [38]). However, it is often more convenient to consider these matrix elements as parameters, which are fitted to reproduce certain properties and can then be used to calculate other properties of the solid (see, for instance, Refs. [39, 40]). We illustrate

these concepts through two simple examples, the first concerning a 1D lattice, the second a 2D lattice of atoms.

4.1.1 Example: 1D linear chain with *s* or *p* orbitals

We consider first the simplest possible case, a linear periodic chain of atoms. Our system has only one type of atom and only one orbital associated with each atom. The first task is to construct the basis for the crystal wavefunctions using the atomic wavefunctions, as was done for the general case in Eq. (4.2). We notice that because of the simplicity of the model, there are no summations over the indices l (there is only one type of orbital for each atom) and i (there is only one atom per unit cell). We keep the index l to identify different types of orbitals in our simple model. Therefore, the basis for the crystal wavefunctions in this case will be simply

$$\chi_{kl}(x) = \sum_{n=-\infty}^{\infty} \mathrm{e}^{\mathrm{i}kx} \phi_l(x - na) \tag{4.12}$$

where we have further simplified the notation since we are dealing with a 1D example, with the position vector $\mathbf{r}$ set equal to the position x on the 1D axis and the reciprocal-space vector $\mathbf{k}$ set equal to k, while the lattice vectors $\mathbf{R}$ are given by na, with a the lattice constant and n an integer. We will consider atomic wavefunctions $\phi_l(x)$ which have either s-like or p-like character. The real parts of the wavefunction $\chi_{kl}(x)$, $l = s, p$ for a few values of k are shown in Fig. 4.1.

With these states, we can now attempt to calculate the band structure for this model. The TBA with an orthogonal basis and nearest neighbor interactions only implies that the overlap matrix elements are non-zero only for orbitals $\phi_l(x)$ on the same atom, that is,

$$\langle \phi_l(x) | \phi_l(x - na) \rangle = \delta_{n0} \tag{4.13}$$

Similarly, nearest neighbor interactions require that the hamiltonian matrix elements are non-zero only for orbitals that are on the same or neighboring atoms. If the orbitals are on the same atom, then we define the hamiltonian matrix element to be

$$\langle \phi_l(x) | \mathcal{H}^{sp} | \phi_l(x - na) \rangle = \epsilon_l \delta_{n0} \tag{4.14}$$

while if they are on neighboring atoms, that is $n = \pm 1$, we define the hamiltonian matrix element to be

$$\langle \phi_l(x) | \mathcal{H}^{sp} | \phi_l(x - na) \rangle = t_l \delta_{n\pm 1} \tag{4.15}$$

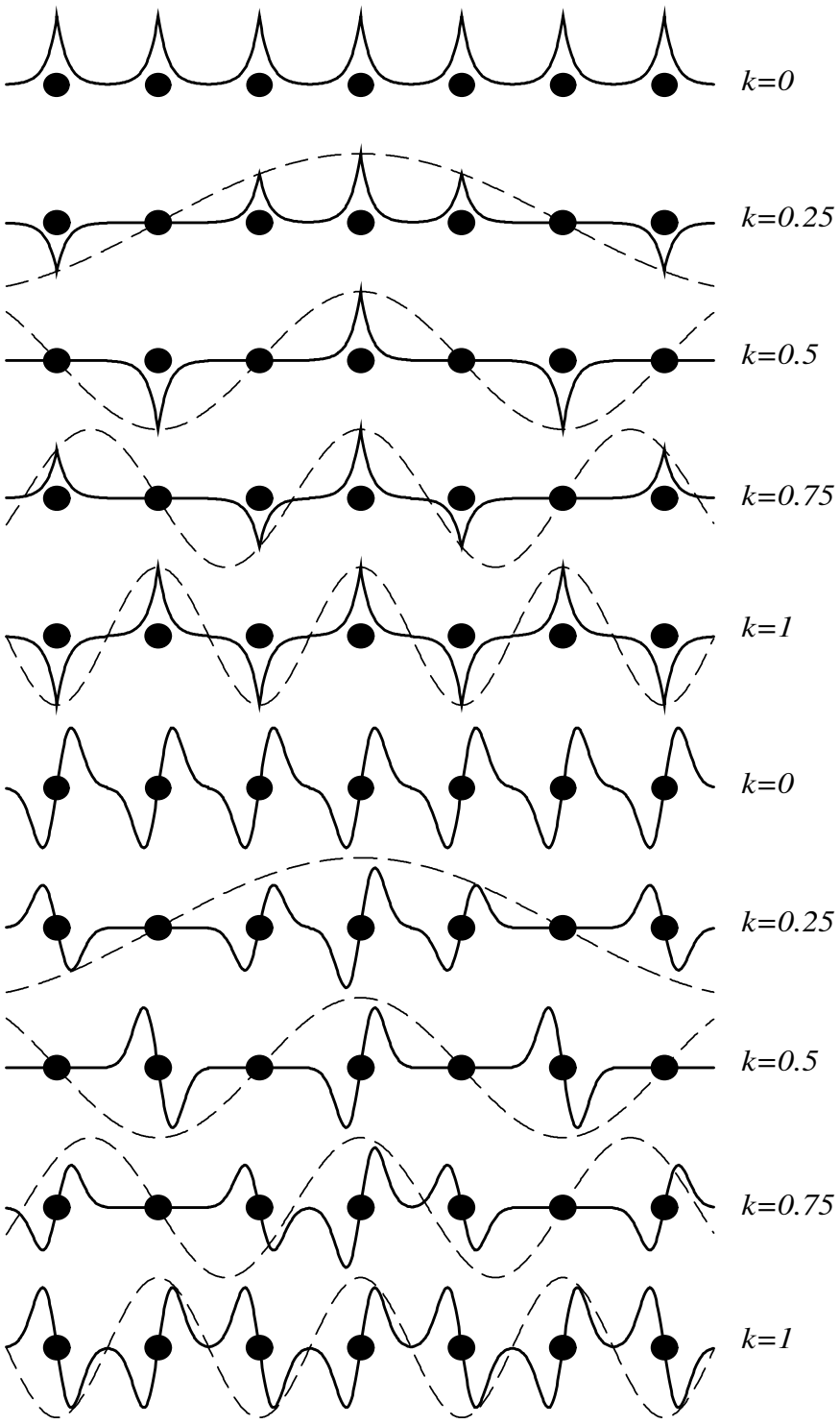

Figure 4.1. Real parts of the crystal wavefunctions $\chi_{kl}(x)$ for $k = 0$, 0.25, 0.5, 0.75 and 1 (in units of π/a); the dashed lines represent the term $\cos(kx)$, which determines the value of the phase factor when evaluated at the atomic sites $x = na$. Top five: s-like state; bottom five: p-like state. The solid dots represent the atoms in the one-dimensional chain.

where ϵ_l is the on-site hamiltonian matrix element and t_l is the hopping matrix element. We expect this interaction between orbitals on neighboring atoms to contribute to the cohesion of the solid, which implies that $t_s < 0$ for s-like orbitals and $t_p > 0$ for p-like orbitals, as we explain in more detail below.

We are now ready to use the $\chi_{kl}(x)$ functions as the basis to construct crystal wavefunctions and with these calculate the single-particle energy eigenvalues, that is, the band structure of the model. The crystal wavefunctions are obtained from the general expression Eq. (4.4):

$$\psi_k(x) = c_k \chi_{kl}(x) \tag{4.16}$$

where only the index k has survived due to the simplicity of the model (the index l simply denotes the character of the atomic orbitals). Inserting these wavefunctions into the secular equation, Eq. (4.5), we find that we have to solve a 1×1 matrix, because we have only one orbital per atom and one atom per unit cell. With the above definitions of the hamiltonian matrix elements between the atomic orbitals ϕ_l's, we obtain

$$\begin{aligned}
&[\langle \chi_{kl}(x)|\mathcal{H}^{sp}|\chi_{kl}(x)\rangle - \epsilon_k \langle \chi_{kl}(x)|\chi_{kl}(x)\rangle]c_k = 0 \\
&\quad \Rightarrow \sum_n \mathrm{e}^{\mathrm{i}kna}\langle \phi_l(x)|\mathcal{H}^{sp}|\phi_l(x-na)\rangle = \epsilon_k \sum_n \mathrm{e}^{\mathrm{i}kna}\langle \phi_l(x)|\phi_l(x-na)\rangle \\
&\quad\quad \Rightarrow \sum_n \mathrm{e}^{\mathrm{i}kna}[\epsilon_l \delta_{n0} + t_l \delta_{n\pm 1}] = \epsilon_k \sum_n \mathrm{e}^{\mathrm{i}kna}\delta_{n0}
\end{aligned}$$

The solution to the last equation is straightforward, giving the energy band for this simple model:

$$\text{1D chain}: \quad \epsilon_k = \epsilon_l + 2t_l \cos(ka) \tag{4.17}$$

The behavior of the energy in the first BZ of the model, that is, for $-\pi/a \leq k \leq \pi/a$, is shown in Fig. 4.2 for the s and p orbitals. Since the coefficient c_k is undefined by the secular equation, we can take it to be unity, in which case the crystal wavefunctions $\psi_k(x)$ are the same as the basis functions $\chi_{kl}(x)$, which we have already discussed above (see Fig. 4.1).

We elaborate briefly on the sign of the hopping matrix elements and the dispersion of the bands. It is assumed that the single-particle hamiltonian is spherically symmetric. The s orbitals are spherically symmetric and have everywhere the same sign,[2] so that the overlap between s orbitals situated at nearest neighbor sites is positive. In order to produce an attractive interaction between these orbitals, the hopping matrix element must be negative:

$$t_s \equiv \int \phi_s^*(x)\mathcal{H}^{sp}(x)\phi_s(x-a)\mathrm{d}x < 0.$$

[2] We are concerned here with the sign implied only by the angular momentum character of the wavefunction and not by the radial part; of the latter part, only the tail beyond the core is involved, as discussed in chapter 2.

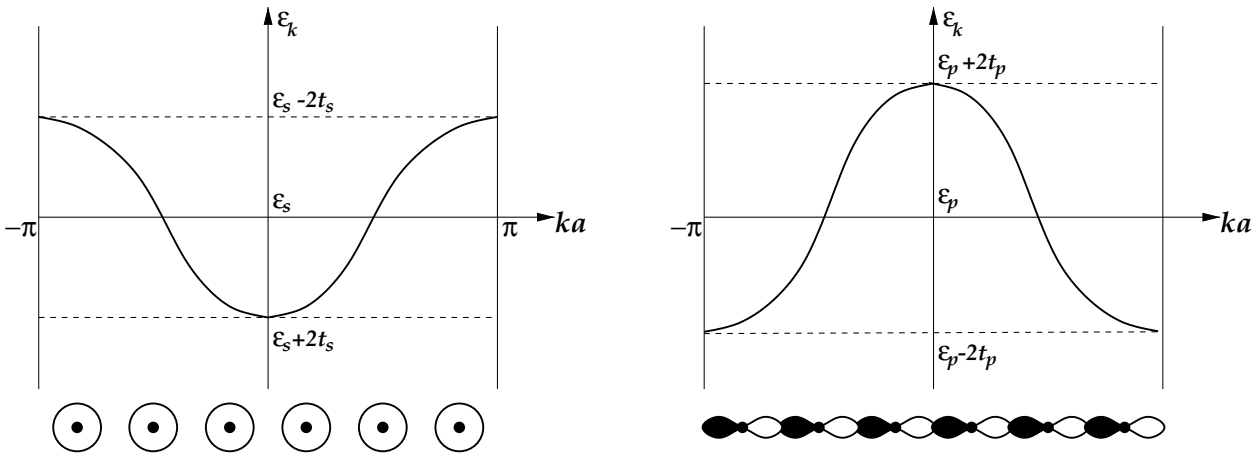

Figure 4.2. Single-particle energy eigenvalues ϵ_k in the first BZ ($-\pi \leq ka \leq \pi$), for the 1D infinite chain model, with one atom per unit cell and one orbital per atom, in the tight-binding approximation with nearest neighbor interactions. **Left:** s-like state; **right:** p-like state. ϵ_s, ϵ_p are the on-site hamiltonian matrix elements and $t_s < 0$ and $t_p > 0$ are the hopping matrix elements. The sketches at the bottom of each panel illustrate the arrangement of the orbitals in the 1D lattice with the positions of the atoms shown as small black dots and the positive and negative lobes of the p orbitals shown in white and black. Due to larger overlap we expect $|t_s| < |t_p|$, which leads to larger dispersion for the p band.

We conclude that the negative sign of this matrix element is due to the hamiltonian, since the product of the wavefunctions is positive. On the other hand, the p orbitals have a positive and a negative lobe (see Appendix B); consequently, the overlap between p orbitals situated at nearest neighbor sites and oriented in the same sense as required by translational periodicity, is negative, because the positive lobe of one is closest to the negative lobe of the next. Therefore, in order to produce an attractive interaction between these orbitals, and since the hamiltonian is the same as in the previous case, the hopping matrix element must be positive

$$t_p \equiv \int \phi_p^*(x)\mathcal{H}^{sp}(x)\phi_p(x-a)\mathrm{d}x > 0.$$

Thus, the band structure for a 1D model with one s-like orbital per unit cell will have a maximum at $k = \pm\pi/a$ and a minimum at $k = 0$, while that of the p-like orbital will have the positions of the extrema reversed, as shown in Fig. 4.2. Moreover, we expect that in general there will be larger overlap between the neighboring p orbitals than between the s orbitals, due to the directed lobes of the former, and therefore $|t_p| > |t_s|$, leading to larger dispersion for the p bands.

The generalization of the model to a two-dimensional square lattice with either one s-like orbital or one p-like orbital per atom and one atom per unit cell is

straightforward; the energy eigenvalues are given by

$$\text{2D square}: \quad \epsilon_{\mathbf{k}} = \epsilon_l + 2t_l[\cos(k_x a) + \cos(k_y a)] \tag{4.18}$$

with the two-dimensional reciprocal-space vector defined as $\mathbf{k} = k_x\hat{\mathbf{x}} + k_y\hat{\mathbf{y}}$. Similarly, the generalization to the three-dimensional cubic lattice with either one s-like orbital or one p-like orbital per atom and one atom per unit cell leads to the energy eigenvalues:

$$\text{3D cube}: \quad \epsilon_{\mathbf{k}} = \epsilon_l + 2t_l[\cos(k_x a) + \cos(k_y a) + \cos(k_z a)] \tag{4.19}$$

where $\mathbf{k} = k_x\hat{\mathbf{x}} + k_y\hat{\mathbf{y}} + k_z\hat{\mathbf{z}}$ is the three-dimensional reciprocal-space vector. From these expressions, we can immediately deduce that for this simple model the band width of the energy eigenvalues is given by

$$W = 4dt_l = 2zt_l \tag{4.20}$$

where d is the dimensionality of the model ($d = 1, 2, 3$ in the above examples), or, equivalently, z is the number of nearest neighbors ($z = 2, 4, 6$ in the above examples). We will use this fact in chapter 12, in relation to disorder-induced localization of electronic states.

4.1.2 Example: 2D square lattice with s and p orbitals

We next consider a slightly more complex case, the two-dimensional square lattice with one atom per unit cell. We assume that there are four atomic orbitals per atom, one s-type and three p-type (p_x, p_y, p_z). We work again within the orthogonal basis of orbitals and nearest neighbor interactions only, as described by the equations of Table 4.1. The overlap matrix elements in this case are

$$\begin{aligned}
&\langle\phi_m(\mathbf{r})|\phi_l(\mathbf{r}-\mathbf{R})\rangle = \delta_{lm}\delta(\mathbf{R}) \\
&\quad\Rightarrow \langle\chi_{\mathbf{k}m}|\chi_{\mathbf{k}l}\rangle = \sum_{\mathbf{R}} \mathrm{e}^{\mathrm{i}\mathbf{k}\cdot\mathbf{R}}\langle\phi_m(\mathbf{r})|\phi_l(\mathbf{r}-\mathbf{R})\rangle = \sum_{\mathbf{R}} \mathrm{e}^{\mathrm{i}\mathbf{k}\cdot\mathbf{R}}\delta_{lm}\delta(\mathbf{R}) \\
&\qquad\qquad = \delta_{lm}
\end{aligned} \tag{4.21}$$

while the hamiltonian matrix elements are

$$\begin{aligned}
&\langle\phi_m(\mathbf{r})|\mathcal{H}^{sp}|\phi_l(\mathbf{r}-\mathbf{R})\rangle \neq 0 \ \text{ only for } \ [\mathbf{R} = \pm a\hat{\mathbf{x}}, \pm a\hat{\mathbf{y}}, 0] \\
&\quad\Rightarrow \langle\chi_{\mathbf{k}m}|\mathcal{H}^{sp}|\chi_{\mathbf{k}l}\rangle = \sum_{\mathbf{R}} \mathrm{e}^{\mathrm{i}\mathbf{k}\cdot\mathbf{R}}\langle\phi_m(\mathbf{r})|\mathcal{H}^{sp}|\phi_l(\mathbf{r}-\mathbf{R})\rangle \\
&\qquad\qquad \neq 0 \ \text{ only for } \ [\mathbf{R} = \pm a\hat{\mathbf{x}}, \pm a\hat{\mathbf{y}}, 0]
\end{aligned} \tag{4.22}$$

There are a number of different on-site and hopping matrix elements that are generated from all the possible combinations of $\phi_m(\mathbf{r})$ and $\phi_l(\mathbf{r})$ in Eq. (4.22),

which we define as follows:

$$
\begin{aligned}
\epsilon_s &= \langle \phi_s(\mathbf{r}) | \mathcal{H}^{sp} | \phi_s(\mathbf{r}) \rangle \\
\epsilon_p &= \langle \phi_{p_x}(\mathbf{r}) | \mathcal{H}^{sp} | \phi_{p_x}(\mathbf{r}) \rangle = \langle \phi_{p_y}(\mathbf{r}) | \mathcal{H}^{sp} | \phi_{p_y}(\mathbf{r}) \rangle = \langle \phi_{p_z}(\mathbf{r}) | \mathcal{H}^{sp} | \phi_{p_z}(\mathbf{r}) \rangle \\
V_{ss} &= \langle \phi_s(\mathbf{r}) | \mathcal{H}^{sp} | \phi_s(\mathbf{r} \pm a\hat{\mathbf{x}}) \rangle = \langle \phi_s(\mathbf{r}) | \mathcal{H}^{sp} | \phi_s(\mathbf{r} \pm a\hat{\mathbf{y}}) \rangle \\
V_{sp} &= \langle \phi_s(\mathbf{r}) | \mathcal{H}^{sp} | \phi_{p_x}(\mathbf{r} - a\hat{\mathbf{x}}) \rangle = -\langle \phi_s(\mathbf{r}) | \mathcal{H}^{sp} | \phi_{p_x}(\mathbf{r} + a\hat{\mathbf{x}}) \rangle \\
V_{sp} &= \langle \phi_s(\mathbf{r}) | \mathcal{H}^{sp} | \phi_{p_y}(\mathbf{r} - a\hat{\mathbf{y}}) \rangle = -\langle \phi_s(\mathbf{r}) | \mathcal{H}^{sp} | \phi_{p_y}(\mathbf{r} + a\hat{\mathbf{y}}) \rangle \\
V_{pp\sigma} &= \langle \phi_{p_x}(\mathbf{r}) | \mathcal{H}^{sp} | \phi_{p_x}(\mathbf{r} \pm a\hat{\mathbf{x}}) \rangle = \langle \phi_{p_y}(\mathbf{r}) | \mathcal{H}^{sp} | \phi_{p_y}(\mathbf{r} \pm a\hat{\mathbf{y}}) \rangle \\
V_{pp\pi} &= \langle \phi_{p_y}(\mathbf{r}) | \mathcal{H}^{sp} | \phi_{p_y}(\mathbf{r} \pm a\hat{\mathbf{x}}) \rangle = \langle \phi_{p_x}(\mathbf{r}) | \mathcal{H}^{sp} | \phi_{p_x}(\mathbf{r} \pm a\hat{\mathbf{y}}) \rangle \\
V_{pp\pi} &= \langle \phi_{p_z}(\mathbf{r}) | \mathcal{H}^{sp} | \phi_{p_z}(\mathbf{r} \pm a\hat{\mathbf{x}}) \rangle = \langle \phi_{p_z}(\mathbf{r}) | \mathcal{H}^{sp} | \phi_{p_z}(\mathbf{r} \pm a\hat{\mathbf{y}}) \rangle
\end{aligned}
\tag{4.23}
$$

The hopping matrix elements are shown schematically in Fig. 4.3. By the symmetry of the atomic orbitals we can deduce:

$$
\begin{aligned}
\langle \phi_s(\mathbf{r}) | \mathcal{H}^{sp} | \phi_{p_\alpha}(\mathbf{r}) \rangle &= 0 \quad (\alpha = x, y, z) \\
\langle \phi_s(\mathbf{r}) | \mathcal{H}^{sp} | \phi_{p_\alpha}(\mathbf{r} \pm a\hat{\mathbf{x}}) \rangle &= 0 \quad (\alpha = y, z) \\
\langle \phi_{p_\alpha}(\mathbf{r}) | \mathcal{H}^{sp} | \phi_{p_\beta}(\mathbf{r} \pm a\hat{\mathbf{x}}) \rangle &= 0 \quad (\alpha, \beta = x, y, z; \alpha \neq \beta) \\
\langle \phi_{p_\alpha}(\mathbf{r}) | \mathcal{H}^{sp} | \phi_{p_\beta}(\mathbf{r}) \rangle &= 0 \quad (\alpha, \beta = x, y, z; \alpha \neq \beta)
\end{aligned}
\tag{4.24}
$$

as can be seen by the diagrams in Fig. 4.3, with the single-particle hamiltonian $\mathcal{H}^{sp}$ assumed to contain only spherically symmetric terms.

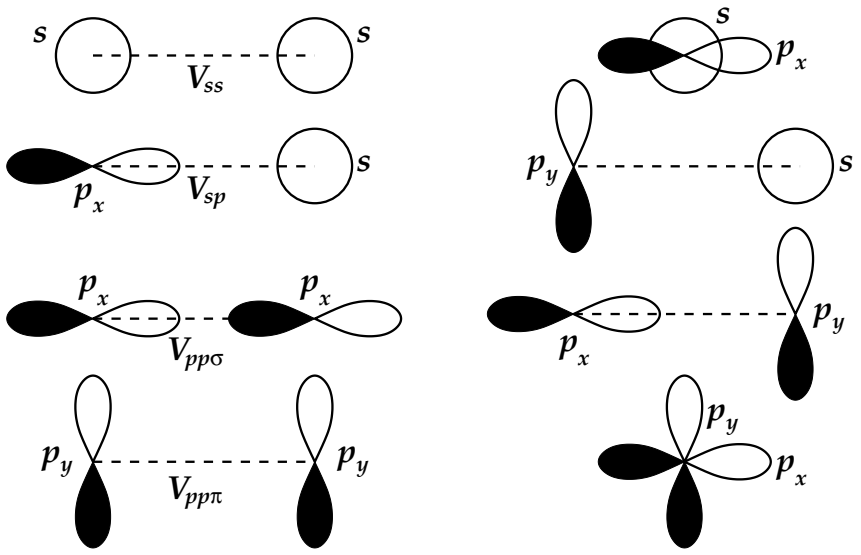

Figure 4.3. Schematic representation of hamiltonian matrix elements between s and p states. **Left:** elements that do not vanish; **right:** elements that vanish due to symmetry. The two lobes of opposite sign of the p_x, p_y orbitals are shaded black and white.

Having defined all these matrix elements, we can calculate the matrix elements between crystal states that enter in the secular equation; we find for our example

$$\begin{aligned}\langle\chi_{\mathbf{k}s}(\mathbf{r})|\mathcal{H}^{sp}|\chi_{\mathbf{k}s}(\mathbf{r})\rangle &= \langle\phi_s(\mathbf{r})|\mathcal{H}^{sp}|\phi_s(\mathbf{r})\rangle \\ &\quad + \langle\phi_s(\mathbf{r})|\mathcal{H}^{sp}|\phi_s(\mathbf{r}-a\hat{\mathbf{x}})\rangle e^{i\mathbf{k}\cdot a\hat{\mathbf{x}}} \\ &\quad + \langle\phi_s(\mathbf{r})|\mathcal{H}^{sp}|\phi_s(\mathbf{r}+a\hat{\mathbf{x}})\rangle e^{-i\mathbf{k}\cdot a\hat{\mathbf{x}}} \\ &\quad + \langle\phi_s(\mathbf{r})|\mathcal{H}^{sp}|\phi_s(\mathbf{r}-a\hat{\mathbf{y}})\rangle e^{i\mathbf{k}\cdot a\hat{\mathbf{y}}} \\ &\quad + \langle\phi_s(\mathbf{r})|\mathcal{H}^{sp}|\phi_s(\mathbf{r}+a\hat{\mathbf{y}})\rangle e^{-i\mathbf{k}\cdot a\hat{\mathbf{y}}} \\ &= \epsilon_s + 2V_{ss}\big[\cos(k_x a)+\cos(k_y a)\big] \end{aligned} \tag{4.25}$$

and similarly for the rest of the matrix elements

$$\begin{aligned}\langle\chi_{\mathbf{k}s}(\mathbf{r})|\mathcal{H}^{sp}|\chi_{\mathbf{k}p_x}(\mathbf{r})\rangle &= 2iV_{sp}\sin(k_x a) \\ \langle\chi_{\mathbf{k}s}(\mathbf{r})|\mathcal{H}^{sp}|\chi_{\mathbf{k}p_y}(\mathbf{r})\rangle &= 2iV_{sp}\sin(k_y a) \\ \langle\chi_{\mathbf{k}p_z}(\mathbf{r})|\mathcal{H}^{sp}|\chi_{\mathbf{k}p_z}(\mathbf{r})\rangle &= \epsilon_p + 2V_{pp\pi}\big[\cos(k_x a)+\cos(k_y a)\big] \\ \langle\chi_{\mathbf{k}p_x}(\mathbf{r})|\mathcal{H}^{sp}|\chi_{\mathbf{k}p_x}(\mathbf{r})\rangle &= \epsilon_p + 2V_{pp\sigma}\cos(k_x a) + 2V_{pp\pi}\cos(k_y a) \\ \langle\chi_{\mathbf{k}p_y}(\mathbf{r})|\mathcal{H}^{sp}|\chi_{\mathbf{k}p_y}(\mathbf{r})\rangle &= \epsilon_p + 2V_{pp\pi}\cos(k_x a) + 2V_{pp\sigma}\cos(k_y a) \end{aligned} \tag{4.26}$$

With these we can now construct the hamiltonian matrix for each value of $\mathbf{k}$, and obtain the eigenvalues and eigenfunctions by diagonalizing the secular equation.

For a quantitative discussion of the energy bands we will concentrate on certain portions of the BZ, which correspond to high-symmetry points or directions in the IBZ. Using the results of chapter 3 for the IBZ for the high-symmetry points for this lattice, we conclude that we need to calculate the band structure along $\Gamma-\Delta-X-Z-M-\Sigma-\Gamma$. We find that at $\Gamma=(k_x,k_y)=(0,0)$, the matrix is already diagonal and the eigenvalues are given by

$$\epsilon_\Gamma^{(1)} = \epsilon_s + 4V_{ss},\ \epsilon_\Gamma^{(2)} = \epsilon_p + 4V_{pp\pi},\ \epsilon_\Gamma^{(3)} = \epsilon_\Gamma^{(4)} = \epsilon_p + 2V_{pp\pi} + 2V_{pp\sigma} \tag{4.27}$$

The same is true for the point $M=(1,1)(\pi/a)$, where we get

$$\epsilon_M^{(1)} = \epsilon_M^{(3)} = \epsilon_p - 2V_{pp\pi} - 2V_{pp\sigma},\ \epsilon_M^{(2)} = \epsilon_p - 4V_{pp\pi},\ \epsilon_M^{(4)} = \epsilon_s - 4V_{ss} \tag{4.28}$$

Finally, at the point $X=(1,0)(\pi/a)$ we have another diagonal matrix with eigenvalues

$$\epsilon_X^{(1)} = \epsilon_p + 2V_{pp\pi} - 2V_{pp\sigma},\ \epsilon_X^{(2)} = \epsilon_p, \epsilon_X^{(3)} = \epsilon_s, \epsilon_X^{(4)} = \epsilon_p - 2V_{pp\pi} + 2V_{pp\sigma} \tag{4.29}$$

We have chosen the labels of those energy levels to match the band labels as displayed on p. 135 in Fig. 4.4(a). Notice that there are doubly degenerate states at

Table 4.2. *Matrix elements for the 2D square lattice with s, p_x, p_y, p_z orbitals at the high-symmetry points Δ, Z, Σ.*

In all cases, $0 < k < 1$.

$\mathbf{k}$	$\Delta = (k, 0)(\pi/a)$	$Z = (1, k)(\pi/a)$	$\Sigma = (k, k)(\pi/a)$
$A_{\mathbf{k}}$	$2V_{ss}(\cos(k\pi) + 1)$	$2V_{ss}(\cos(k\pi) - 1)$	$4V_{ss}\cos(k\pi)$
$B_{\mathbf{k}}$	$2\mathrm{i}V_{sp}\sin(k\pi)$	$2\mathrm{i}V_{sp}\sin(k\pi)$	$2\sqrt{2}\mathrm{i}V_{sp}\sin(k\pi)$
$C_{\mathbf{k}}$	$2V_{pp\sigma}\cos(k\pi) + 2V_{pp\pi}$	$2V_{pp\sigma}\cos(k\pi) - 2V_{pp\pi}$	$2(V_{pp\sigma} + V_{pp\pi})\cos(k\pi)$
$D_{\mathbf{k}}$	$2V_{pp\sigma} + 2V_{pp\pi}\cos(k\pi)$	$2V_{pp\pi}\cos(k\pi) - 2V_{pp\sigma}$	$2(V_{pp\sigma} + V_{pp\pi})\cos(k\pi)$
$E_{\mathbf{k}}$	$2V_{pp\pi}(\cos(k\pi) + 1)$	$2V_{pp\pi}(\cos(k\pi) - 1)$	$4V_{pp\pi}\cos(k\pi)$

Γ and at M, dictated by symmetry, that is, by the values of $\mathbf{k}$ at those points and the form of the hopping matrix elements within the nearest neighbor approximation. For the three other high-symmetry points, Δ, Z, Σ, we obtain matrices of the type

$$\begin{bmatrix} A_{\mathbf{k}} & B_{\mathbf{k}} & 0 & 0 \\ B_{\mathbf{k}}^* & C_{\mathbf{k}} & 0 & 0 \\ 0 & 0 & D_{\mathbf{k}} & 0 \\ 0 & 0 & 0 & E_{\mathbf{k}} \end{bmatrix} \tag{4.30}$$

The matrices for Δ and Z can be put in this form straightforwardly, while the matrix for Σ requires a change of basis in order to be brought into this form, namely

$$\begin{aligned} \chi_{\mathbf{k}1}(\mathbf{r}) &= \frac{1}{\sqrt{2}}\left[\chi_{\mathbf{k}p_x}(\mathbf{r}) + \chi_{\mathbf{k}p_y}(\mathbf{r})\right] \\ \chi_{\mathbf{k}2}(\mathbf{r}) &= \frac{1}{\sqrt{2}}\left[\chi_{\mathbf{k}p_x}(\mathbf{r}) - \chi_{\mathbf{k}p_y}(\mathbf{r})\right] \end{aligned} \tag{4.31}$$

with the other two functions, $\chi_{\mathbf{k}s}(\mathbf{r})$ and $\chi_{\mathbf{k}p_z}(\mathbf{r})$, the same as before. The different high-symmetry $\mathbf{k}$-points result in the matrix elements tabulated in Table 4.2. These matrices are then easily solved for the eigenvalues, giving:

$$\epsilon_{\mathbf{k}}^{(1,2)} = \frac{1}{2}\left[(A_{\mathbf{k}} + C_{\mathbf{k}}) \pm \sqrt{(A_{\mathbf{k}} - C_{\mathbf{k}})^2 + 4|B_{\mathbf{k}}|^2}\right],\ \epsilon_{\mathbf{k}}^{(3)} = D_{\mathbf{k}},\ \epsilon_{\mathbf{k}}^{(4)} = E_{\mathbf{k}} \tag{4.32}$$

We have then obtained the eigenvalues for all the high-symmetry points in the IBZ. All that remains to be done is to determine the numerical values of the hamiltonian matrix elements.

In principle, one can imagine calculating the values of the hamiltonian matrix elements using one of the single-particle hamiltonians we discussed in chapter 2. There is a question as to what exactly the appropriate atomic basis functions $\phi_l(\mathbf{r})$ should be. States associated with free atoms are not a good choice, because in

the solid the corresponding single-particle states are more compressed due to the presence of other electrons nearby. One possibility then is to solve for atomic-like states in fictitious atoms where the single-particle wavefunctions are compressed, by imposing for instance a constraining potential (typically a harmonic well) in addition to the Coulomb potential of the nucleus.

Alternatively, one can try to guess the values of the hamiltonian matrix so that they reproduce some important features of the band structure, which can be determined independently from experiment. Let us try to predict at least the sign and relative magnitude of the hamiltonian matrix elements, in an attempt to guess a set of reasonable values. First, the diagonal matrix elements ϵ_s, ϵ_p should have a difference approximately equal to the energy difference of the corresponding eigenvalues in the free atom. Notice that if we think of the atomic-like functions $\phi_l(\mathbf{r})$ as corresponding to compressed wavefunctions then the corresponding eigenvalues ϵ_l are not identical to those of the free atom, but we could expect the compression of eigenfunctions to have similar effects on the different eigenvalues. Since the energy scale is arbitrary, we can choose ϵ_p to be the zero of energy and ϵ_s to be lower in energy by approximately the energy difference of the corresponding free-atom states. The choice $\epsilon_s = -8$ eV is representative of this energy difference for several second row elements in the Periodic Table.

The matrix element V_{ss} represents the interaction of two $\phi_s(\mathbf{r})$ states at a distance a, the lattice constant of our model crystal. We expect this interaction to be attractive, that is, to contribute to the cohesion of the solid. Therefore, by analogy to our earlier analysis for the 1D model, we expect V_{ss} to be negative. The choice $V_{ss} = -2$ eV for this interaction would be consistent with our choice of the difference between ϵ_s and ϵ_p. Similarly, we expect the interaction of two p states to be attractive in general. In the case of $V_{pp\sigma}$ we are assuming the neighboring $\phi_{p_x}(\mathbf{r})$ states to be oriented along the x axis in the same sense, that is, with positive lobes pointing in the positive direction as required by translational periodicity. This implies that the negative lobe of the state to the right is closest to the positive lobe of the state to the left, so that the overlap between the two states will be negative. Because of this negative overlap, $V_{pp\sigma}$ should be positive so that the net effect is an attractive interaction, by analogy to what we discussed earlier for the 1D model. We expect this matrix element to be roughly of the same magnitude as V_{ss} and a little larger in magnitude, to reflect the larger overlap between the directed lobes of p states. A reasonable choice is $V_{pp\sigma} = +2.2$ eV. In the case of $V_{pp\pi}$, the two p states are parallel to each other at a distance a, so we expect the attractive interaction to be a little weaker than in the previous case, when the orbitals were pointing toward each other. A reasonable choice is $V_{pp\pi} = -1.8$ eV. Finally, we define V_{sp} to be the matrix element with $\phi_{p_x}(\mathbf{r})$ to the left of $\phi_s(\mathbf{r})$, so that the positive lobe of the p orbital is closer to the s orbital and their overlap is positive. As a consequence

Table 4.3. *Values of the on-site and hopping matrix elements for the band structure of the 2D square lattice with an orthogonal s and p basis and nearest neighbor interactions.*

ϵ_p is taken to be zero in all cases. All values are in electronvolts. (a)–(f) refer to parts in Fig. 4.4.

	(a)	(b)	(c)	(d)	(e)	(f)
ϵ_s	−8.0	−16.0	−8.0	−8.0	−8.0	−8.0
V_{ss}	−2.0	−2.0	−4.0	−2.0	−2.0	−2.0
$V_{pp\sigma}$	+2.2	+2.2	+2.2	+4.4	+2.2	+2.2
$V_{pp\pi}$	−1.8	−1.8	−1.8	−1.8	−3.6	−1.8
V_{sp}	−2.1	−2.1	−2.1	−2.1	−2.1	−4.2

of this definition, this matrix element, which also contributes to attraction, must be negative; we expect its magnitude to be somewhere between the V_{ss} and $V_{pp\sigma}$ matrix elements. A reasonable choice is $V_{sp} = -2.1$ eV. With these choices, the model yields the band structure shown in Fig. 4.4(a). Notice that in addition to the doubly degenerate states at Γ and M which are expected from symmetry, there is also a doubly degenerate state at X; this is purely accidental, due to our choice of parameters, as the following discussion also illustrates.

In order to elucidate the influence of the various matrix elements on the band structure we also show in Fig. 4.4 a number of other choices for their values. To keep the comparisons simple, in each of the other choices we increase one of the matrix elements by a factor of 2 relative to its value in the original set and keep all other values the same; the values for each case are given explicitly in Table 4.3. The corresponding Figs. 4.4 (b)–(f) provide insight into the origin of the bands. To facilitate the comparison we label the bands 1–4, according to their order in energy near Γ.

Comparing Figs. 4.4 (a) and (b) we conclude that band 1 arises from interaction of the s orbitals in neighboring atoms: a decrease of the corresponding eigenvalue ϵ_s from −8 to −16 eV splits this band off from the rest, by lowering its energy throughout the BZ by 8 eV, without affecting the other three bands, except for some minor changes in the neighborhood of M where bands 1 and 3 were originally degenerate. Since in plot (b) band 1 has split from the rest, now bands 3 and 4 have become degenerate at M, because there must be a doubly degenerate eigenvalue at M independent of the values of the parameters, as we found in Eq. (4.28). An increase of the magnitude of V_{ss} by a factor of 2, which leads to the band structure of plot (c), has as a major effect the increase of the dispersion of band 1; this confirms that band 1 is primarily due to the interaction between s orbitals. There are also some changes in band 4, which at M depends on the value of V_{ss}, as found in Eq. (4.28).

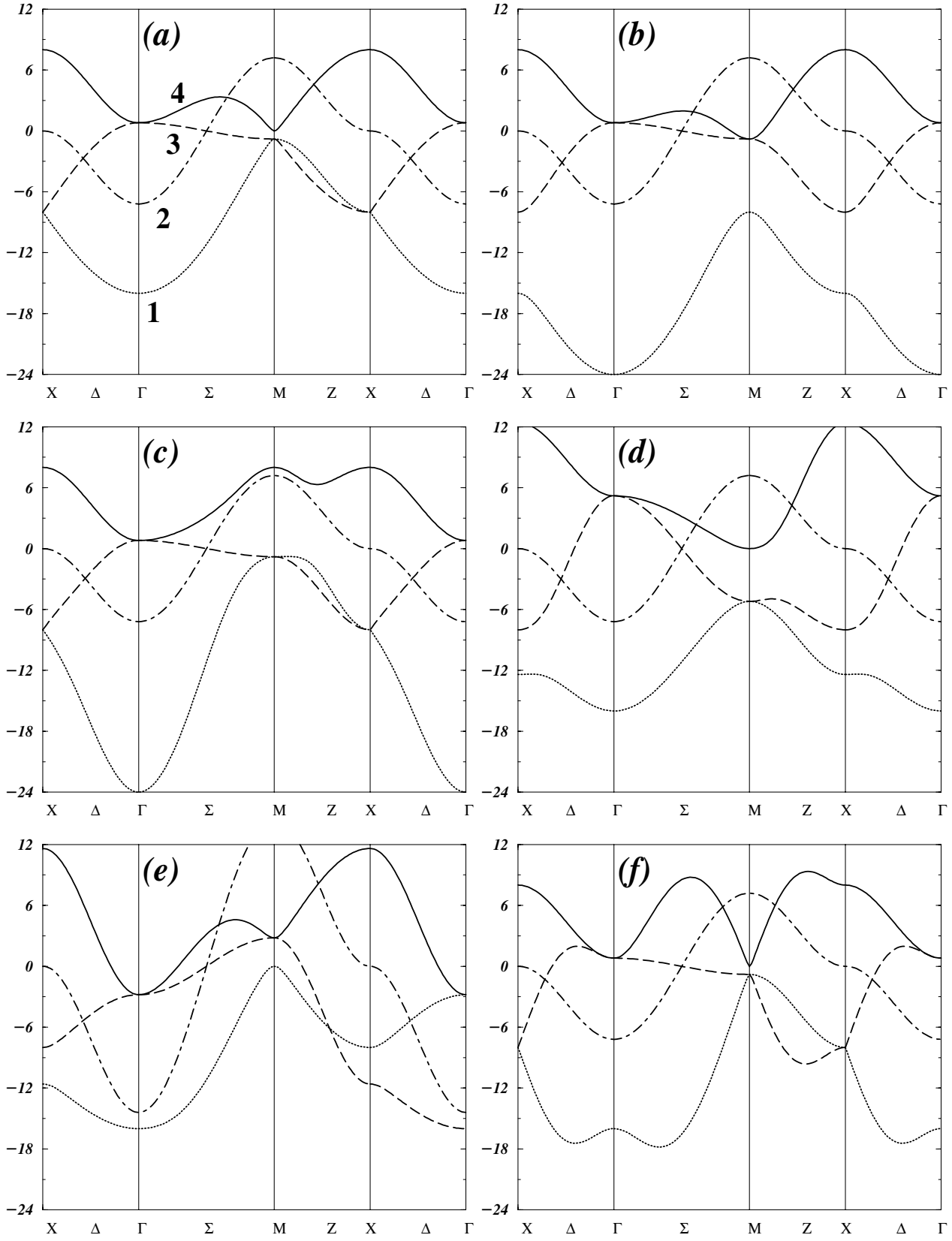

Figure 4.4. The band structure of the 2D square lattice with one atom per unit cell and an orthogonal basis consisting of s, p_x, p_y, p_z orbitals with nearest neighbor interactions. The values of the parameters for the six different plots are given in Table 4.3.

Increasing the magnitude of $V_{pp\sigma}$ by a factor of 2 affects significantly bands 3 and 4, somewhat less band 1, and not at all band 2, as seen from the comparison between plots (a) and (d). This indicates that bands 3 and 4 are essentially related to σ interactions between the p_x and p_y orbitals on neighboring atoms. This is also supported by plot (e), in which increasing the magnitude of $V_{pp\pi}$ by a factor of 2 has as a major effect the dramatic increase of the dispersion of band 2; this leads to the conclusion that band 2 arises from π-bonding interactions between p_z orbitals. The other bands are also affected by this change in the value of $V_{pp\pi}$, because they contain π-bonding interactions between p_x and p_y orbitals, but the effect is not as dramatic, since in the other bands there are also contributions from σ-bonding interactions, which lessen the importance of the $V_{pp\pi}$ matrix element. Finally, increasing the magnitude of V_{sp} by a factor of 2 affects all bands except band 2, as seen in plot (f); this is because all other bands except band 2 involve orbitals s and p interacting through σ bonds.

Two other features of the band structure are also worth mentioning: First, that bands 1 and 3 in Figs. 4.4(a) and (b) are nearly parallel to each other throughout the BZ. This is an accident related to our choice of parameters for these two plots, as the other four plots prove. This type of behavior has important consequences for the optical properties, as discussed in chapter 5, particularly when the lower band is occupied (it lies entirely below the Fermi level) and the upper band is empty (it lies entirely above the Fermi level). The second interesting feature is that the lowest band is parabolic near Γ, in all plots of Fig. 4.4 except for (f). The parabolic nature of the lowest band near the minimum is also a feature of the simple 1D model discussed in section 4.1.1, as well as of the free-electron model discussed in chapter 3. In all these cases, the lowest band near the minimum has essentially pure s character, and its dispersion is dictated by the periodicity of the lattice rather than interaction with other bands. Only for the choice of parameters in plot (f) is the parabolic behavior near the minimum altered; in this case the interaction between s and p orbitals (V_{sp}) is much larger than the interaction between s orbitals, so that the nature of the band near the minimum is not pure s any longer but involves also the p states. This last situation is unusual. Far more common is the behavior exemplified by plots (a) – (d), where the nature of the lowest band is clearly associated with the atomic orbitals with the lowest energy. This is demonstrated in more realistic examples later in this chapter.

4.1.3 Generalizations of the TBA

The examples we have discussed above are the simplest version of the TBA, with only orthogonal basis functions and nearest neighbor interactions, as defined in Eq. (4.21) and Eq. (4.22), respectively. We also encountered matrix elements in